Spherical Foot Placement Estimator for Humanoid Balance Control and Recovery

Brandon J. DeHart, Rob Gorbet, and Dana Kulić

Abstract— **One of the main challenges of bipedal gait is to avoid falling due to unknown disturbances. Compensating for these disturbances in bipeds is often achieved by leaning or stepping. In this work, the Spherical Foot Placement Estimator (SFPE) is introduced, which uses the biped's current kinematics and dynamics to predict if a step is needed, and if so where to step, to restore balance in 3D. An example of a controller using the SFPE is shown, which augments an existing optimal controller with both leaning and stepping: SFPE-based feedback is used to generate a desired momentum for momentum-based leaning while the SFPE point is used as a control reference for stepping. The new estimator outperforms existing balance criteria by providing both recovery step location prediction and momentum objectives with smooth dynamics.**

I. Introduction

A critical capability for humanoid robots is to maintain or recover balance using disturbance compensation methods, which mainly fall into three categories: flexing, leaning, and stepping. In this work, we focus on the leaning and stepping approaches to disturbance compensation.

Leaning uses changes in posture to counteract moderate disturbances, generally by using momentum-based control [1]–[6]. *Stepping* consists of lifting a foot and planting it in a new location, sometimes repeatedly, to compensate for larger disturbances [6]–[9]. There is a large body of existing work on disturbance compensation using stepping or leaning approaches, although most work assumes that the biped is at rest when disturbed [1]–[6]. Less work has been done which combines these approaches [6], [7].

Stepping methods typically use *balance point estimators*, which identify a *balance point* (or *points*) where the robot can step to restore balance. Here, we introduce a novel 3D balance point estimator, called the Spherical Foot Placement Estimator (SFPE), which extends the planar Foot Placement Estimator (FPE) [10] and its existing 3D extensions [6], [11]. This novel estimator has been developed to address the drawbacks of existing balance point estimators, and can be used to determine if a biped is going to lose its balance, how to compensate, and where to step if a step is needed.

The SFPE is predictive, considers impact, includes rotational inertia, allows ankle torques and 3D Center of Mass (COM) motion, does not require flat ground or heuristic parameters, and works for a biped at rest or in motion. We develop the SFPE equations and compare it to other balance point estimators in simulation (including other 3D extensions of the FPE) using a simple COM feedback controller. We then show how to modify this simple controller to use the SFPE to improve a biped's dynamic balance.

*This work was supported by the Natural Sciences and Engineering Research Council and the Ontario Graduate Scholarship Program.

Brandon J. DeHart and Dana Kulić are with the Department of Electrical & Computer Engineering, University of Waterloo, Ontario, Canada.

Rob Gorbet is with the Department of Knowledge Integration, University of Waterloo, Ontario, Canada.

{bjdehart,rbgorbet,dana.kulic}@uwaterloo.ca

A. Related Work

There are two high-level categories of balance point estimators: those which include the effects of impact and those that do not. The Linear Inverted Pendulum Model (LIPM) [12] is used in the majority of methods that ignore impact.

The LIPM assumes (often horizontal) planar COM motion, consists of a telescoping pendulum between the COM and the Center of Pressure (COP), and ignores rotational inertia about the COM. It is used to find the Instantaneous Capture Point (ICP) [13]: the point where a biped should step (if the LIPM assumptions hold) so that the COM comes to rest.

The Divergent Component of Motion (DCM) can be thought of as the 3D analog of the ICP, since its ground projection is located at the ICP (on horizontal ground) [14]. Recently, Englsberger et al. have made use of the DCM for planning COM motions from a desired footstep plan using the Centroidal Moment Pivot (CMP) point, along with heuristic step-based balancing [9] and analytical footstep adjustment for recovery from strong disturbances [15]. These disturbance compensation methods assume no change in angular momentum and no dynamic effects due to impact.

The (impact-based) Foot Placement Estimator [10] calculates where a 2D compass-gait biped should step such that its COM comes to rest directly above the newly placed foot. Cho *et al.* used a closed form version of the FPE for successful foot placement of a hopping HUBO2 robot [16]. Two 3D extensions of the FPE concept have been proposed: the Generalized FPE (GFPE) [6] and the 3D FPE [11].

The GFPE [6] uses a 2D rimless spoked wheel model to predict a recovery step location, based on the velocity of the COM after a biped at rest is pushed. The model is embedded in a vertical plane (containing the COM) parallel to the COM velocity, and uses a modified version of the original planar FPE formulations for step prediction. However, the GFPE neglects the rotational inertia of the biped about the COM, and assumes that the biped is at rest before a disturbance.

The 3D FPE [11] applies the original FPE in a vertical plane (containing the COM) perpendicular to the horizontal components of the biped's angular momentum about the ground projection of the COM. Like the original FPE, the 3D FPE does not require the biped to be at rest nor in contact with the ground before impact. However, it is only defined

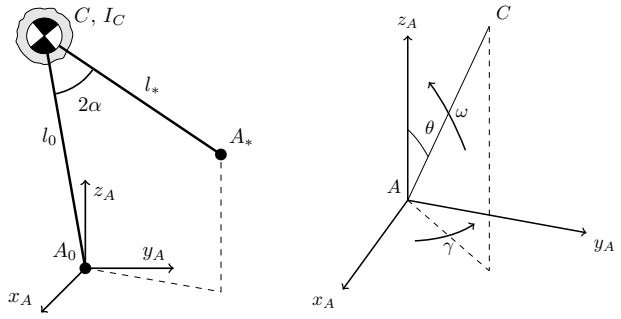

(a) Diagram of the SFPE's 3D rimless spoked wheel model.

(b) Diagram of the spherical coordinates used for the SFPE.

Fig. 1. Diagrams of the SFPE model and coordinates. The model in (a) shows that the COM, C, is used as the attachment point of two legs with point feet. Note that the model used in this work includes a rotational inertia about C, labeled I_C. In (b), the spherical coordinates centered at the anchor point, A, are used to describe the motion of the COM, C. Note that θ is always measured in a vertical plane which contains both C and A and the distance between C and A, the leg length l, is assumed to be constant.

for horizontal ground surfaces and is not predictive, requiring continuous calculation until impact occurs.

When using the 3D FPE, the full 3D dynamics of a biped are projected into the assumed (vertical) 3D FPE impact plane, to determine its planar rotational inertia and average angular velocity. The SFPE defined in Section II is a novel 3D formulation of the FPE which projects the full 3D dynamics into both a vertical impact plane and a horizontal plane and uses a rimless wheel for predictive purposes, combining and extending the GFPE and 3D FPE.

II. Spherical Foot Placement Estimator

Similar to the GFPE, the SFPE uses a rimless wheel model, with two fixed length legs attached at the COM, C, and a leg separation of 2α (see Figure 1a). It is assumed that only one of the model's point feet is in contact with the ground at any given time, allowing them to be labeled based on the state of the model: A_0, the current anchor foot (on the ground), and A_*, the future anchor foot.

When a step is taken, A_* is assumed to land on the ground without slipping or bouncing at the same instant as A_0 lifts off the ground, causing the status (and therefore labels) of the feet to switch instantaneously. By assuming a fixed leg length between C and each anchor point, the motion of C can be described by a series of piecewise rotations about successive anchor points, replacing the common assumption of planar motion of the COM. This assumption produces a more realistic COM path, as typically the COM of a biped follows smoothed inverted pendular curves in 3D, not motion in successive (approximately horizontal) planes [17].

Thanks to this assumption of purely spherical motion of C during each step, spherical coordinates centered at each successive anchor point are used to define the model's dynamics in terms of three variables (see Figure 1b): the angle between the leg and the vertical axis, θ; its derivative, $\omega = \dot{\theta}$; and the angular velocity of C about the same vertical axis, γ. We assume no rotation about the stance leg axis.

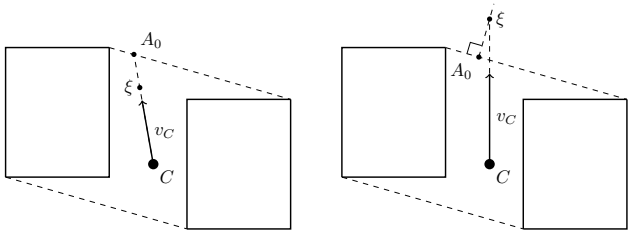

(a) How to choose A_0 when the DCM is above the SP.

(b) How to choose A_0 when the DCM is not above the SP.

Fig. 2. Illustrations of how to select the anchor point location, A_0. When the Divergent Component of Motion (DCM), ξ, is above the biped's convex support polygon (SP), A_0 is chosen as the (furthest) intersection of the perimeter of the SP with a ground-projected vector from C through ξ, as shown in (a). If ξ is not above the biped's SP, A_0 is chosen as the point on the edge of the SP closest to the ground projection of ξ, as shown in (b).

These variables define the motion of the COM of the simplified model about the given anchor point, based on the linear velocity of the COM of the full multibody system. The simplified model includes only a single rigid body with its COM at the COM of the full system, which is constrained to 2D rotation about the anchor point.

Unlike the GFPE, the model used in this work moves in 3D and includes rotational inertia about the COM, labeled I_C. This rotational inertia is the rotational submatrix of the biped's centroidal inertia matrix (the Composite Rigid Body matrix for the biped evaluated at the COM [5]). Multiplying the inverse of the centroidal inertia matrix by the centroidal momentum of the biped, the system's COM velocity v_C and average angular velocity ω_C can also be calculated [5].

For the purposes of generating a predictive balance point, we select a pair of planes (one vertical and one horizontal) which approximate the motion of the 3D model. The planar inertia of the simple model in both of these planes is estimated using the I_C matrix (similar to the projection used to generate the 3D FPE in [8], [11]).

The height of the horizontal plane and the location and rotation of the vertical plane require the definition of an appropriate anchor point for the simplified model. For the SFPE, the anchor point A_0 is chosen to represent the location of maximum effectiveness for the Centroidal Moment Pivot point (CMP), as shown in Figure 2.

As discussed in [9], the dynamics of the Divergent Component of Motion (DCM) can be controlled using the CMP, as the DCM always moves directly away from the CMP. Therefore, placing the CMP on the edge of a biped's convex support polygon (SP) in the direction of v_C will produce maximum deceleration of the COM (if the DCM is above the SP). Similiarly, as described in [7], once the instantaneous Capture Point (ICP) has exited a biped's SP, maintaining the CMP as close as possible to the ICP is found to minimize the number of steps required to recover.

Unlike the COP or projected COP, which is used in the GFPE and may be discontinuous, this choice of anchor point will vary smoothly with changes in C and v_C, and is more likely to be the point around which C will be purely

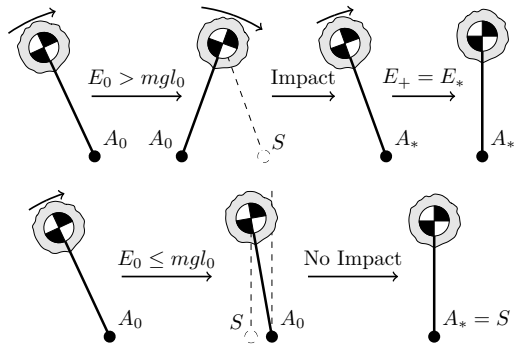

Fig. 3. Illustration of the possible state transitions of the SFPE model. The top row illustrates the case where the initial energy is high enough to overcome the potential energy well created by the rigid leg, requiring a step. In this case, the legs are assumed to be equal in length and a balance point, S, is determined which, when stepped on by a swinging foot, will result in C stopping above S. If the energy is not high enough to require a step, the bottom row of state transitions applies. In this case, the swinging leg length is $l_* = E_0/mg$ and therefore is only equal to l_0 when $E_0 = mgl_0$.

rotating once a step is needed. When a step is required, this anchor point also provides the ability to correct for small disturbances (internal or external) without affecting the predicted SFPE point (assuming the stance foot is fixed), by moving the COP around within the support polygon.

In the development of the SFPE, several specific instants in the progression of the simplified model's state ($x = [\theta\ \omega\ \gamma]$) are used, and are labeled with the following subscripts:

- 0 The current state of the model,
- $-$ Just before the landing foot impacts the ground,
- $+$ Just after the landing foot impacts the ground, and
- $*$ The final state of the model

As shown in Figure 3, there are several possible state transitions when using the SFPE. If a step is not required, an SFPE point is defined within the biped's SP which can be used to predict COM motion (as discussed in Section II-A). Otherwise, finding the SFPE point requires a set of equations which relate the current state of the biped (x_0) to its final state (x_*), which are separated into three categories:

- Pre-impact equations, relating x_0 to x_-;
- Impact equations, relating x_- to x_+; and
- Post-impact equations, relating x_+ to x_*.

These three sets of equations are defined in Sections II-B to II-D, using conservation of energy and/or momentum, as appropriate. The SFPE point S is then found as the point which satisfies these equations and results in the desired final state: in these examples, with C at rest above S.

A. Core Equations

The rotational inertia of the model is estimated for the two planes introduced above, where I_C^ω and I_C^γ are defined as the estimates of I_C in the vertical ω and horizontal γ planes, respectively. Using these definitions, the angular momenta estimates about A (in the two planes) are

$$k^\omega(\omega) = (I_C^\omega + ml^2)\omega = I^\omega\omega \tag{1}$$

$$k^\gamma(\theta,\gamma) = (I_C^\gamma + ml^2\sin^2(\theta))\gamma = I^\gamma(\theta)\gamma \tag{2}$$

The estimated kinetic energy $T(\theta,\omega,\gamma) = T^\omega(\omega) + T^\gamma(\theta,\gamma)$ can therefore be written as

$$T = \frac{1}{2}I^\omega\omega^2 + \frac{1}{2}I^\gamma\gamma^2 = \frac{(k^\omega)^2}{2I^\omega} + \frac{(k^\gamma)^2}{2I^\gamma} \tag{3}$$

Writing the potential energy as $U(\theta) = mgl\cos\theta$, we can then write the system's total estimated energy as

$$E(\theta,\omega,\gamma) = T^\omega(\omega) + T^\gamma(\theta,\gamma) + U(\theta) \tag{4}$$

If C is above the support polygon, then there is the possibility that a given disturbance doesn't require the biped to step, but simply to shift its CMP. If the current estimated energy of the model, E_0, is no more than the maximum potential energy ($E_0 \leq mgl_0$), then no step is required (assuming full control over the CMP) [18].

In this case, the balance point S is defined as the closest point the COM ground projection G will reach, relative to the edge of the SP, if the CMP is held at A_0. This is found by setting the final leg length l_* to the maximum height C will reach above A_0, $l_* = E_0/mg$, and applying trigonometry to determine the distance d_{MIN} from G to A_0 at that height (using the constant leg length l_0 between C and A_0). S is the point between the current G and A_0 which is d_{MIN} away from A_0 (see the bottom row of Figure 3).

If a step is required (i.e., $E_0 > mgl_0$), then the three sets of impact equations are required to determine where to step to achieve the desired final state. To simplify these equations, it is assumed that the model's pre- and post-impact leg lengths are equal ($l_0 = l_* = l$) and therefore that all of the above equations can be used at all instants in question.

As was done in the original FPE method (and its extensions), at each time step the current inertia of the multibody system is used to estimate the fixed inertia of the simplified model. For the SFPE, this means the planar inertia estimates for the two planes of motion (I_C^ω and I_C^γ) are assumed to be constant at the three critical instants for prediction purposes. The predicted location of the SFPE balance point is recalculated at each time step using the current inertial and dynamic properties of the multibody system, instead of making one prediction just after the disturbance.

B. Pre-Impact Equations

Pre-impact equations enable prediction of where the biped will need to step at some point in the future to recover its balance, by defining x_- in terms of the current state, x_0.

In [10] and [11], it was assumed that a foot could be instantaneously placed anywhere on the ground, and therefore that $x_0 = x_-$. In [6] and [19], conservation of energy was used to determine the pre-impact equations, although they assumed vertical planar rotation about the COP (or its projection) and ignored the biped's rotational inertia.

Our assumption of spherical motion about A_0 leads to a formulation using conservation of energy and conservation of angular momentum to determine the pre-impact state, x_-.

Since gravity cannot create a torque about a vertical axis and no active torque is applied about the vertical axis, k^γ around that axis is a conserved quantity. Based on this, the

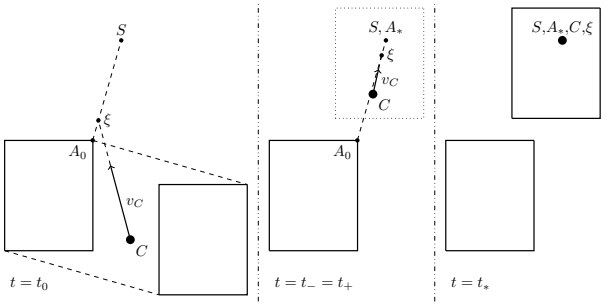

Fig. 4. Illustrations showing a bird's eye view of the vertical plane of impact and the points C, A_0, S, and the DCM ξ. It is clear that although C is not currently in the impact plane defined by A_0 and ξ, that it will be located in the plane (or very close to it) once impact occurs.

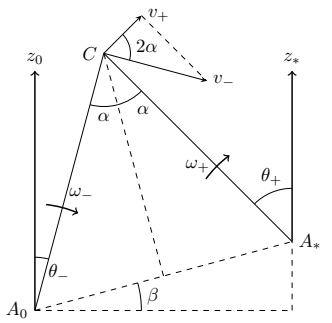

Fig. 5. Illustration of relationship between various angles and points in the impact plane at the moment of impact (assuming C is in plane during impact). Since the leg length is assumed constant, the distance from A_0 to C is equal to the distance from A_* to C. Note that v_- is perpendicular to CA_0, while v_+ is perpendicular to CA_*.

angular momentum around the vertical axis at A_0 prior to impact is assumed to be constant: $k_0^\gamma = k_-^\gamma$.

Defining $T_C^\gamma = (k_0^\gamma)^2/2I_C^\gamma$, we can rewrite $T^\gamma(\theta_-)$ as

$$T_-^\gamma = \frac{(k_-^\gamma)^2}{2I_-^\gamma} = \frac{(k_0^\gamma)^2}{2I_C^\gamma \eta_-} = \frac{T_C^\gamma}{\eta_-} \tag{5}$$

where $\eta(\theta) = 1 + (ml^2/I_C^\gamma)\sin^2\theta$ and $\eta_- = \eta(\theta_-)$.

Conservation of energy is used as the basis of the pre-impact equations by setting the pre-impact energy equal to the current energy (i.e., $E_0 = E_-$). We assume that the values of I_C^ω and I_C^γ, in their respective planes, will have the same value at impact as their current values, and that all current values (those with subscript 0) are known. The only remaining unknowns in the pre-impact equation are the impact angle θ_- and its derivative ω_-.

This leads to an equation for T_-^ω in terms of θ_-, known values E_0 and T_C^γ, and constants:

$$T_-^\omega = E_0 - \frac{T_C^\gamma}{\eta(\theta_-)} - U(\theta_-) \tag{6}$$

C. Impact Equations

Due to the loss of energy during impact, conservation of angular momentum is used to generate the impact equations to relate the pre-impact kinetic energy, T_-, to the post-impact kinetic energy, T_+. The constants used to generate the pre-impact equations are also assumed to remain constant across impact, since there is effectively no change in the model's dynamics other than an instantaneous change in velocity.

The vertical plane in which impact will occur is assumed to currently include both A_0 and the DCM ξ (and, of course, the SFPE balance point S), but not necessarily C, as shown in Figure 4. This ensures that S is calculated relative to where C is heading, as opposed to its current location, as the COM is attracted towards the DCM according to $\xi = C + bv_C$, where b is the time constant of the DCM dynamics [9].

Note that the impact and post-impact equations are being calculated before the future anchor foot lands (i.e., as part of a prediction), so the predicted landing foot location maintains its label (A_*). In the vertical impact plane, the angular momentum around A_* just after impact will be k_+^ω. However, since the model is assumed to be purely rotating about A_0 just prior to impact and about A_* just after impact, $k_+^\omega \neq k_-^\omega$.

To relate k_+^ω to k_-^ω, the standard FPE equations for conservation of angular momentum at impact are used [10]. As shown in Figure 5, due to the geometry of the model the equality $v_+ = \cos(2\alpha)v_- = \cos(2\alpha)lw_-$ holds, so k_+^ω can be written in terms of ω_- as

$$k_+^\omega = I_C^\omega \omega_- + mlv_+ = \left(I_C^\omega + ml^2\cos(2\alpha)\right)\omega_- \tag{7}$$

This leads to the dimensionless impact ratio $\zeta(\alpha)$ relating the pre- and post-impact angular momenta in the ω plane:

$$\zeta = \frac{k_+^\omega}{k_-^\omega} = \frac{(I_C^\omega + ml^2\cos(2\alpha))\omega_-}{I^\omega \omega_-} \tag{8}$$

Therefore, T_+^ω can be written in terms of T_-^ω as:

$$T_+^\omega = \frac{(k_+^\omega)^2}{2I^\omega} = \frac{(\zeta k_-^\omega)^2}{2I^\omega} = \zeta^2 T_-^\omega \tag{9}$$

Using a similar method, the dimensionless inertia ratio $\psi(\theta_-, \theta_+)$ can be written as (using $d(\theta) = l\sin\theta$):

$$\psi = \frac{k_+^\gamma}{k_-^\gamma} = \frac{(I_C^\gamma - md_+d_-)\gamma_-}{I_-^\gamma \gamma_-} \tag{10}$$

Combining this with the asumption of conservation of angular momentum in the horizontal plane leading up to impact (i.e., $k_0^\gamma = k_-^\gamma$) enables us to write T_+^γ as:

$$T_+^\gamma = \frac{(k_+^\gamma)^2}{2I_+^\gamma} = \frac{(\psi k_0^\gamma)^2}{2I_C^\gamma \eta_+} = \psi^2 \frac{T_C^\gamma}{\eta_+} \tag{11}$$

D. Post-Impact Equations

After impact, conservation of energy can again be applied by assuming that the model remains in a fixed configuration and that the desired final angle θ_* and final angular velocity ω_* are known. This builds on the assumptions that the model is in pure rotation about A_* after impact, and that the model's fixed parameters (l, I_C^ω, etc) remain constant.

Based on these assumptions, the model's post-impact equations can be determined in the same way as the pre-impact equations. Conservation of angular momentum in the horizontal plane can be used again to define the equality

$k_+^\gamma = k_*^\gamma$. Using the pre- and post-impact conservation of k^γ and the inertia ratio ψ, we can then write T_*^γ as

$$T_*^\gamma = \frac{(k_*^\gamma)^2}{2I_*^\gamma} = \frac{(\psi k_0^\gamma)^2}{2I_C^\gamma \eta(\theta_*)} = \psi^2 \frac{T_C^\gamma}{\eta_*} \tag{12}$$

which, along with the desired values of θ_* and ω_*, allows us to calculate the final estimated energy $E_* = T_*^\omega + T_*^\gamma + U_*$.

This leads to the post-impact equation, very similar to the pre-impact equation (6), for T_+^ω in terms of only θ_-, θ_+, known values E_* and T_C^γ, and constants:

$$T_+^\omega = E_* - \psi^2(\theta_-, \theta_+)\frac{T_C^\gamma}{\eta(\theta_+)} - U(\theta_+) \tag{13}$$

By combining the pre- and post-impact equations (6) and (13) with the ratios ζ and ψ, the following energy-based SFPE equation in terms of α, θ_-, and θ_+ is produced:

$$E_* - \psi^2 \frac{T_C^\gamma}{\eta_+} - U_+ = \zeta^2 \left(E_0 - \frac{T_C^\gamma}{\eta_-} - U_- \right) \tag{14}$$

To determine the location of S, the θ_- and θ_+ values must be redefined to allow this equation to be in terms of one common angle. As shown in Figure 5, these angles can be defined as $\theta_- = \alpha - \beta$ and $\theta_+ = \alpha + \beta$, where β is the angle between S and a horizontal plane, measured at A_0. For a horizontal planar ground surface, it is easy to show that $\beta = 0$ at all instants, and therefore that $\theta_- = \theta_+ = \alpha$.

For a planar, but not necessarily horizontal, ground surface, β can be easily determined based on the impact plane and the value of α. To determine the angle β for intersecting planar ground surfaces, the methods discussed in [6] can be used to define β as a function of α and the surface slopes. In general, it is assumed β can be defined as a function of α, leading to an equation whose only variable is α.

Solving the SFPE equation for α and applying trigonometry in the impact plane gives the location of S, the SFPE balance point, with respect to the current anchor point A_0.

In general, we assume that the final desired state consists of C held directly above A_*, by setting $\theta_* = 0$ and $\omega_* = 0$. Based on this assumed final state, the final estimated energy E_* is the sum of the final potential energy, $U_* = mgl$, and the final kinetic energy, $T_* = T_*^\gamma = \psi^2 T_C^\gamma$.

Although the SFPE has been developed with this specific final state in mind, an alternative final state would only require modification to the values of θ_* and ω_*. For example, a final state which includes a desired velocity for the COM (e.g., for gait generation purposes) would require setting $\omega_* \neq 0$, and would likely require $\theta_* \neq 0$ as well. See [10] and [8] for examples of the application of the FPE and its extensions for the generation of bipedal gait.

III. Comparison

To clearly show the differences between the SFPE and existing balance point estimators, a simulation of Boston Dynamics' Atlas robot [20] in the MATLAB toolbox Drake [21] was subjected to initial instantaneous velocity disturbances. These initial velocities are similar to the disturbances used in [19] to compare two balance points and the instantaneous velocity changes applied as disturbances in [9]. The optimal controller from [22] (the default Atlas controller in Drake) was slightly modified to take a desired linear momentum as an additional control reference, to be tracked using PD gains on the linear momentum error (see Figure 6a).

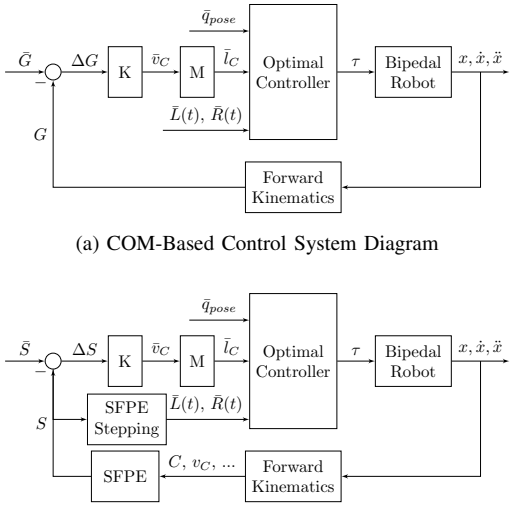

(a) COM-Based Control System Diagram

(b) SFPE-Based Control System Diagram

Fig. 6. System diagrams for the COM-based and SFPE-based control systems. The labelled signals are: τ for torque, v_C for COM velocity, l_C for linear momentum, G for the ground projection of C, S for the SFPE balance point, q_{pose} for postural joint angles, $L(t)$ and $R(t)$ for the foot trajectories, and x for the state (joint angles and 6DOF floating base). Dots over a variable signify a derivative, a bar over a variable signifies a desired value, and a Δ in front of a variable signifies an error. In both of these systems, the optimal controller from [22] is augmented with a linear momentum input, which is calculated using a proportional gain ($K = 5$) on an error term. As shown in (a), for the comparisons in Figure 7 the COM ground projection error was used. For the comparisons in Figure 8, the controller in (b) was used, where the SFPE error was used to generate the linear momentum reference and an SFPE-based stepping controller was included.

The SFPE is formulated to handle piecewise flat ground, similar to the GFPE. However, the results in this work have been generated for flat ground, by setting $\beta = 0$ everywhere. Also, the upper body joints (back, arms, neck) were held static, to allow fair comparisons between criteria that assume a point mass at the COM and those with rotational inertia.

The desired linear momentum of the COM was set in the same way as in [3]–[5], with damping on the COM velocity and the desired COM set to the center of the single supporting foot. The SFPE and other balance points are calculated and graphed at each time step.

Figure 7 illustrates the results and highlights the differences between the balance points: The ICP is purely a function of the COM kinematics and gravity, and therefore is not directly influenced by inertia, angular momentum, or any of the internal system kinematics. The 3D FPE also makes no assumptions about the system's kinematics, but includes an impact model, rotational inertia, and angular momentum in addition to the COM kinematics and gravity.

This effectively means the 3D FPE is an extended form of the ICP, which includes the system's rotational properties and the energy losses due to impact. In these initial comparisons, due to regulation of angular momentum, the 3D FPE tracks

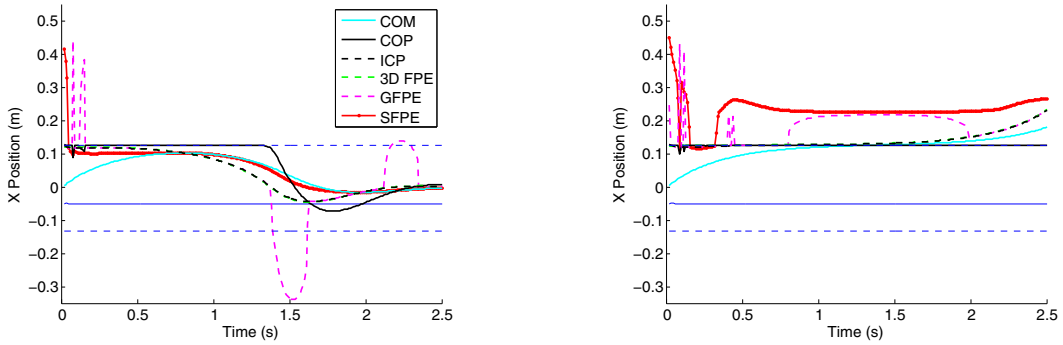

(a) X Disturbance of 0.410 m/s

(b) X Disturbance of 0.420 m/s

Fig. 7. Comparison between the SFPE and other balance points for an Atlas robot [20] when the pelvis is subjected to initial velocity disturbances in the X direction. The values of the velocity disturbances were chosen to illustrate the differences between the balance points and hold no special significance. Smaller velocities cause similar patterns to Figure (a), with the COM remaining closer to the foot center, while larger velocities cause the COM to exit the foot faster. The robot is standing on one foot throughout each simulation, with the ground projection of the ankle shown by a thin blue line, while dashed blue lines show the toe (top) and heel (bottom) of the foot. Since the angular momentum and COM velocity are damped, the 3D FPE point and ICP are approximately equal. Since it has no concept of the support polygon, the GFPE point sometimes predicts a step is required when the system can recover by leaning. Anytime the GFPE does not predict a step is required, the GFPE point is not clearly defined. Here we define it using similar methods as used for the SFPE (see the bottom row of Figure 3). In these simulations, the robot is controlled using the COM-based controller shown in Figure 6a. In (a), the COM-based controller is able to compensate for the disturbance. Since no step is required, the SFPE predicts the location at which the COM could stop, assuming the COP is used to maximum effect (i.e., placed at A_0). Note the SFPE and GFPE points start outside of the foot in both cases, due mainly to their initial kinetic energy assumptions being violated right after the initial disturbance. In (b), the COM-based controller is not able to compensate for the disturbance, and a step is required. Although the SFPE point returns to the foot temporarily, suggesting that a better controller may be able to avoid stepping, it then leaves the SP and quickly predicts a stepping location to recover from the given disturbance. Note that in (b) the 3D FPE point and ICP do not leave the SP until 0.6 s and 0.8 s, respectively, and the GFPE point does not reliably predict a step is needed until 0.8 s and then stops just before 2 s. Also, due to the SFPE including rotational inertia, it predicts a larger step is needed than the GFPE, which only considers a point mass at the COM.

along with the ICP very consistently, confirming this. In general, it is apparent that the exit of the ICP or 3D FPE from the support polygon can be used as a good indicator that the biped will need to take a step in the near future.

However, if a step is required, only the SFPE and GFPE are predictive and can therefore provide a desired landing location ahead of time for the motion planner to generate a suitable trajectory for the swing foot. Although a predictive CP was discussed in [19], it was shown to be a worse step indicator than their predictive FPE-based solution, so was left out of this comparison. Capture regions [7] are also a predictive extension of the ICP, but require flat ground and supply a region in which to step based on a minimum step time instead of a specific location based on COM motion.

As predictive models, the GFPE and SFPE use an anchor point to define the pre-impact equations of motion, which directly influences their associated balance points. The GFPE anchor point is at the orthogonal projection of the COP into the vertical plane used for the GFPE model (described in Section I-A). This means the GFPE anchor point moves due to changes in the relative locations of the ICP, COM, or COP, which causes the GFPE point in Figures 7b and 8a to falsely predict a step is needed when the biped is balanced. This is also the cause of the fluctuations in the GFPE in the figures.

The GFPE equations are not clearly defined when the initial energy is lower than the model's peak potential energy. In this work, we assume this no-step-required GFPE point is defined similarly to the SFPE when no step is required.

Instead of using the projected COP, the SFPE anchor point moves along the edges of the stance foot, which is kinematically fixed (barring foot rotation or slipping) and moves smoothly. Also, when no step is required, an alternative set of equations are defined for its use as a predictive COM reference signal (see Section II-A). During this low energy portion of motion, the SFPE predicts where the COM will stop, assuming a COP at A_0. Unlike the 3D FPE or GFPE, which only consider energy in a vertical plane, the SFPE also takes into consideration the kinetic energy due to motion about a vertical axis, which causes the model's kinetic energy to be both smoother and closer to the real kinetic energy.

IV. SFPE-Based Controller

As a proof of concept, we demonstrate that the SFPE can be used for both leaning and stepping using an example of an SFPE-based controller. This controller uses a proportional gain on the error between the current and desired SFPE points (at each time step) to generate a desired COM velocity, which is then multiplied by the mass of the robot to produce a linear centroidal momentum reference (see Figure 6b).

If the desired SFPE is set as the ground projection of the desired COM location, the key difference between this controller and the COM-based controller is the error term used to generate this linear momentum reference. The new controller uses the error between the predicted future COM ground projection (i.e., the current SFPE) and the desired COM ground projection, as opposed to using the error between the current and desired COM ground projections.

As shown in Figure 8, this momentum reference signal enables the robot to respond to stronger disturbances without losing its balance. The only difference between Figures 7b and 8a is the formulation of the momentum reference which is provided to the CMM controller. This is clearly shown

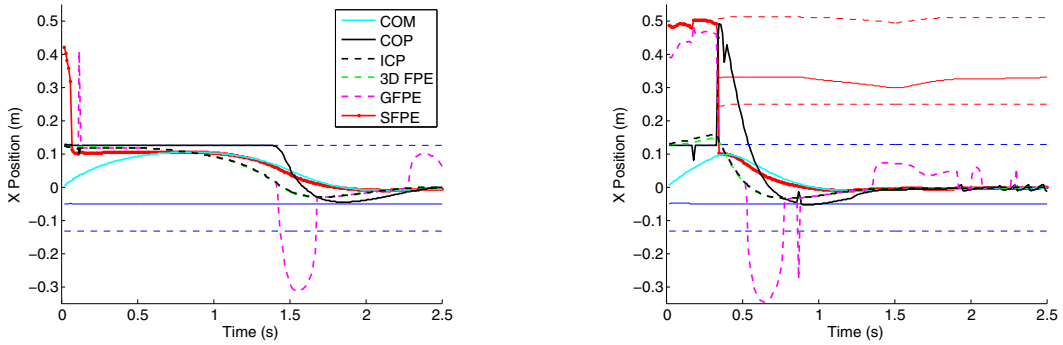

(a) X Disturbance of 0.420 m/s

(b) X Disturbance of 0.430 m/s

Fig. 8. Comparison between the SFPE and other balance points when the pelvis is subjected to large initial velocity disturbances in the X direction, and an SFPE-based controller is used instead of the COM-based controller. Immediately after the disturbances, the SFPE is far from its desired location (the foot center), which causes the controller to generate a desired COM velocity which will bring the SFPE back towards its desired location (as shown in 6b). Note that other than changing the method for generating the reference momentum, the conditions of (a) are identical to those in Figure 7b, including standing in single support at rest before the disturbance. Again, the SFPE and GFPE points start outside of the foot due to their initial kinetic energy assumptions being violated right after the instantaneous velocity disturbance. However, in (b) the SFPE point maintains its position outside the foot over several time steps, so a step is required. The SFPE point is used as a control reference to place the raised foot on the ground (as shown at approximately 0.3 s into the simulation, using dashed red lines for the extents of the right foot and a thin red line for the ground projection of the right ankle). Note that in this case, the COP immediately moves to the toes of the landed foot, moving the SFPE point (and the DCM and COM) back towards the desired location at the center of the original support polygon (the left foot). For larger velocities, a longer step is required but the behavior is qualitatively similar.

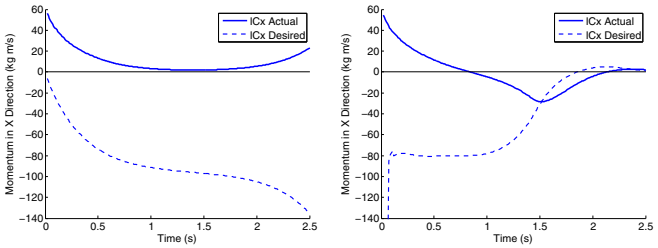

(a) Using COM-Based Controller

(b) Using SFPE-Based Controller

Fig. 9. Comparison between the linear momentum behavior for the COM- and SFPE-based controllers. The results in (a) correspond to Figure 7b, while those shown in (b) correspond to Figure 8a. As shown here, since the SFPE predicts where G will come to rest if the COP is placed at A_0, it can be used to preemptively move the COM backwards.

in the linear momentum graphs of Figure 9, where the immediate reaction of the SFPE-based controller (Figure 6b) allows the biped to remain balanced, while the delayed reaction of the COM-based controller (Figure 6a) does not.

The SFPE controller's response to a larger disturbance is shown in Figure 8b, where even though the controller is able to react immediately, the limitations of balancing solely using the COP are exceeded and, in the absence of other strategies, a step is needed. When taking a step, the controller uses the SFPE point as a control reference to help determine where to place the swinging foot. As shown in Figure 8b, the foot is placed to ensure that the COP can be positioned to allow it to move the SFPE back into the original support polygon.

It should be noted that the robot itself is not constrained to the assumed motion of the simplified pendulum, and in fact departs significantly from the 3D pendulum motion that is predicted using the SFPE's internal model. In fact, evidence of this is clearly shown at the beginning the graphs in Figures 7 and 8, where the SFPE and GFPE points are initially located outside the foot just after the disturbance due to violations of their kinetic energy assumptions.

Much like the FPE point, the SFPE point serves only as an estimate (albeit a reasonably good one) of where the full multibody system should step to come to rest. A dual version of the SFPE with an anchor point at each of the robot's ankles and a corresponding stepping point for each foot was also developed, but was found not to perform as well as the support-polygon-based SFPE that was used in this paper.

A selection of dynamic simulations, including those shown in Figures 7 and 8, can be viewed in the accompanying video.

V. Discussion

The SFPE evaluates the current system dynamics in 3D by finding the current centroidal momentum and inertia and the overall energy of the system. It was designed to address the drawbacks of existing balance point estimators, by incorporating and extending desirable features of the GFPE, 3D FPE, and other methods discussed in Section I-A.

Like the GFPE, the SFPE is predictive and can be applied to piecewise planar ground surfaces. Unlike the GFPE or the predictive estimators in [19], the SFPE also defines a balance point when it does not predict that a step is required, which can be used for leaning control. The SFPE also includes knowledge about the support polygon, instead of using the projected COP anchor point of the GFPE, avoiding false indications that stepping is required when it is not.

Unlike the more common ICP, FPE, and 3D FPE, the SFPE is predictive, which enables it to estimate both when a step is required and where to step ahead of time, allowing time to plan a swing foot trajectory. Although we have previously used the 3D FPE for the control of a biped in [8], the predictive nature of the SFPE and its inclusion of non-flat ground make it the better choice in most cases. This

prediction also incorporates rotation about a vertical axis, which is a novel estimator feature not found in the literature.

The main limitation of the SFPE approach is due to the estimation of the inertia in the two assumed planes of motion, ignoring any intrinsic rotation of the system about the COM, coupled inertia terms, or changes in centroidal inertia, and the assumption of a constant leg length in the simplified model. As discussed in [11], a numerical sensitivy analysis can be conducted to judge the effects of these assumptions.

The original FPE, on which the SFPE and 3DFPE are based, was found to be insensitive to changes in leg length, moment of inertia, or overall energy [11]. A direct effect of these assumptions is the location of the SFPE point being outside of the foot when the system is subject to a large initial velocity disturbance (as seen in Figures 7 and 8).

Some insight into the behavior of a biped at impact can be gained by analyzing the $\zeta(\alpha) = k_+^\omega / k_-^\omega$ inertia ratio of equation (8). The equation can be further simplified, using the trigonometry identity $\cos(2\alpha) = 1 - 2\sin^2\alpha$, to

$$\zeta(\alpha) = 1 - 2(ml^2/I^\omega)\sin^2\alpha \tag{15}$$

By assuming a maximum leg separation of $\pi/2$, the range of α is restricted to $0 \leq \alpha \leq \pi/4$, which leads to the inequality: $0 \leq 2\sin^2\alpha \leq 1$. In other words, the angular velocity of the biped is reduced during impact by the product of the positive inertia ratio, $ml/I^\omega \leq 1$, and a positive scaling factor, $2\sin^2\alpha \leq 1$. Therefore, $0 \leq \zeta(\alpha) \leq 1$.

Effectively, this means that for a given biped which can be approximately modeled as above, the loss of energy at impact is purely a function of the separation angle of the legs, 2α. It also means that if an impulsive force is generated by the biped's stance leg at the moment of impact, which produces an increase in ω_+ equal to the loss due to impact above, the effects of impact on the biped could be ignored. Since the effects of impact are routinely assumed to be negligible in many humanoid control strategies, the equations above could be used to develop a simple controller which might enforce the validity of the lossless-impact assumption.

Finally, a number of existing controllers can benefit from the SFPE, particularly those without the capability to generate footsteps online or which do not control momentum. For example, the optimal controller from [22] (Drake's default Atlas controller) was augmented with linear momentum feedback using the SFPE (see Figure 6b), enabling an easy combination of their pre-planned movements with online compensation while adding minor additional complexity.

VI. Conclusion

In this work, a novel balance point estimator called the Spherical Foot Placement Estimator has been introduced. It has been formulated to overcome a number of drawbacks of existing balance point estimators, by combining and extending desirable features of several different balance points.

The SFPE was compared to other balance point estimators, and was shown to outperform them by providing recovery step location prediction and momentum objectives with smooth dynamics. An SFPE-based feedback loop was used in a momentum-based controller as an example of how to add leaning to an existing whole-body controller and a dynamic SFPE-based stepping strategy was used to deal with large disturbances, demonstrating its utility in bipedal control.

Future work will include examinations of varying leg lengths, changing rotational inertia, experiments on a variety of sloped/varying terrain, and the generation of other possible formulations of the pre-impact equations to produce a more general SFPE. A comparison of the SFPE to more balance point estimators is also left to future work, either directly or via integrated controllers designed for this purpose.

References

[1] S.-H. Hyon, "Compliant Terrain Adaptation for Biped Humanoids Without Measuring Ground Surface and Contact Forces," *IEEE Trans. Robot.*, vol. 25, no. 1, pp. 171–178, 2009.

[2] S.-H. Hyon, R. Osu, and Y. Otaka, "Integration of multi-level postural balancing on humanoid robots," in *ICRA*, 2009, pp. 1549–1556.

[3] S.-H. Lee and A. Goswami, "Ground reaction force control at each foot: A momentum-based humanoid balance controller for non-level and non-stationary ground," in *IROS*, 2010, pp. 3157–3162.

[4] S.-H. Lee and A. Goswami, "A momentum-based balance controller for humanoid robots on non-level and non-stationary ground," *Auton. Robots*, vol. 33, no. 4, pp. 399–414, apr 2012.

[5] D. E. Orin, A. Goswami, and S.-H. Lee, "Centroidal dynamics of a humanoid robot," *Auton. Robots*, vol. 35, pp. 161–176, 2013.

[6] S.-k. Yun and A. Goswami, "Momentum-based reactive stepping controller on level and non-level ground for humanoid robot push recovery," in *IROS*, 2011, pp. 3943–3950.

[7] T. Koolen *et al.*, "Capturability-based analysis and control of legged locomotion, Part 1: Theory and application to three simple gait models," *Int. J. Rob. Res.*, vol. 31, no. 9, pp. 1094–1113, jul 2012.

[8] B. J. DeHart and D. Kulić, "Push Recovery and Online Gait Generation for 3D Bipeds with the Foot Placement Estimator," in *ICRA*, 2014, pp. 1937–1942.

[9] J. Englsberger, C. Ott, and A. Albu-Schaffer, "Three-Dimensional Bipedal Walking Control Based on Divergent Component of Motion," *IEEE Trans. Robot.*, vol. 31, no. 2, pp. 355–368, 2015.

[10] D. L. Wight, E. G. Kubica, and D. W. L. Wang, "Introduction of the Foot Placement Estimator: A Dynamic Measure of Balance for Bipedal Robotics," *J. Comput. Nonlinear Dyn.*, vol. 3, no. 1, p. 011009, 2008.

[11] M. Millard, J. McPhee, and E. Kubica, "Foot Placement and Balance in 3D," *J. Comput. Nonlinear Dyn.*, vol. 7, no. 2, p. 021015, 2012.

[12] S. Kajita *et al.*, "The 3D Linear Inverted Pendulum Mode: A simple modeling for a biped walking pattern generation," in *IROS*, 2001, pp. 239 – 246.

[13] J. Pratt *et al.*, "Capture Point: A Step toward Humanoid Push Recovery," in *HUMANOIDS*, 2006, pp. 200–207.

[14] T. Takenaka, T. Matsumoto, and T. Yoshiike, "Real time motion generation and control for biped robot -1st report: Walking gait pattern generation-," in *IROS*, 2009, pp. 1084–1091.

[15] J. Englsberger, G. Mesesan, and C. Ott, "Smooth trajectory generation and push-recovery based on Divergent Component of Motion," in *IROS*, 2017, pp. 4560–4567.

[16] B.-K. Cho, J.-H. Kim, and J.-H. Oh, "Balancing Strategy using the Principle of Energy Conservation for a Hopping Humanoid Robot," *Int. J. Humanoid Robot.*, vol. 10, no. 3, 2013.

[17] M. S. Orendurff *et al.*, "The effect of walking speed on center of mass displacement." *J. Rehabil. Res. Dev.*, vol. 41(6A), pp. 829–834, 2004.

[18] Z. Li *et al.*, "Fall Prediction of Legged Robots Based on Energy State and Its Implication of Balance Augmentation: A Study on the Humanoid," in *ICRA*, 2015, pp. 5094–5100.

[19] Z. Li *et al.*, "Comparison Study of Two Inverted Pendulum Models for Balance Recovery," in *HUMANOIDS*, 2014, pp. 67–72.

[20] Boston Dynamics, "Boston Dynamics' Atlas Robot," 2017. [Online]. Available: http://www.bostondynamics.com/atlas

[21] R. Tedrake and the Drake Development Team, "Drake: A planning, control, and analysis toolbox for nonlinear dynamical systems," 2016. [Online]. Available: http://drake.mit.edu

[22] S. Kuindersma, F. Permenter, and R. Tedrake, "An Efficiently Solvable Quadratic Program for Stabilizing Dynamic Locomotion," in *ICRA*, 2014, pp. 2589–2594.